SCIENCE CHINA
Technological Sciences

• Article •

November 2016 Vol.59 No.11: 1696–1706
doi: 10.1007/s11431-016-0205-5

Coupling mechanism of mathematical models for sediment transport based on characteristic theory

DING Yun[1], LI ZuiSen[2*], ZHONG DeYu[3] & KANG YanPing[4]

[1] *State Key Laboratory of Hydrology-Water Resources and Hydraulic Engineering, Hohai University, Nanjing 210098, China;*
[2] *Zhejiang Institute of Hydraulics and Estuary, Hangzhou 310008, China;*
[3] *State Key Laboratory of Hydroscience and Engineering, Tsinghua University, Beijing 100084, China;*
[4] *Jiangsu Hydraulic Research Institute, Nanjing 210017, China*

Received March 16, 2016; accepted June 29, 2016; published online August 16, 2016

This paper aims to explore the coupling mechanism between flow movement, sediment transport and riverbed evolution in currently widely used mathematical models for sediment transport. Based on characteristic theory, analytic forms of eigenvalues, eigenvectors and characteristic relationships of total-sediment transport model, bed-load transport model and suspened-load transport model were derived, respectively. The singular perturbation technology was implemented to obtain the asymptotic solutions to different families of eigenvalues. The results indicate that, interactions between motion variables were explicitly coupled in the characteristics of total-sediment transport model and bed-load transport model. Further qualitative and quantitative analysis demonstrates that high sediment transport intensity and significant riverbed change will inevitably affect the property of flow movement. In the process of deposition, sediment-laden flow will move faster when sediment transport intensity becomes stronger. In contrast, the wave of flow will propagate at slower speed as erosion intensity becomes stronger. For most existing suspended-load transport models, however, the characteristics are decoupled as the interactions between motion variables cannot be integrally illustrated in eigenvalues, eigenvectors and characteristic relationship.

coupling mechanism, mathematical models, sediment transport, characteristics, eigenvalues

Citation: Ding Y, Li Z S, Zhong D Y, et al. Coupling mechanism of mathematical models for sediment transport based on characteristic theory. Sci China Tech Sci, 2016, 59: 1696–1706, doi: 10.1007/s11431-016-0205-5

1 Introduction

Over the recent decades, physically based mathematical models have been widely used to the simulation of sediment transport and morphological evolution. A large number of models for sediment transport have been developed and can be found in the literature [1–9]. These models can overall be classified into total-sediment transport models, bed-load sediment models and suspended-load transport models, according to the property of sediment movement.

In addition, most of existing models for sediment transport can be classified into three different types, according to the solution procedure employed: fully coupled models, semicoupled models, and decoupled models [10]. Decoupled models adopt the assumption that the morphological changes are negligible within a computational time step, and the terms of sediment transport and bed mobility in flow equations are ignored [11,12]. Decoupled models are commonly used as they have the available numerical facilities because of the low computing cost. Semicoupled models solve the governing equations for flow and sediment transport together by method of iteration. In a given time step, riverbed evolution is initially predicted by the flow

*Corresponding author (email: lizuisen@hotmail.com)

variables obtained previously and then flow variables are adjusted by the new bed level. These steps of iteration are repeated until the differences between successive estimates of variables arrive at a minor value [13,14]. Fully coupled models solve the flow equations together with the sediment continuity equation simultaneously in a given time step [4, 15–19].

With the development of numerical simulation, many researchers have realized drawbacks existing in sediment transport models [10,11,20–26]. The main drawbacks could be ascribed to the "fixed-bed" assumption that the rate of bed morphological evolution is of a lower order of magnitude compared to flow with adequately low sediment concentration [12,15]. Therefore, the bed mobility is commonly neglected in the simplified flow continuity equation, whilst spatial variations in suspended sediment concentration and momentum transfer due to sediment exchange between the flow and the erodible bed are commonly neglected in the flow momentum equations. In many practical cases in which riverbed evolution is weak and is with a lower order of magnitude than that of flow, the assumptions are reasonable. However, in simulation of rapid and significant riverbed evolution (e.g. dam-break flows, hyperconcentrated flooding and strong tidal currents), application of decoupled models may lead to unacceptable problems, mainly because the coupling between flow motion, sediment transport and bed evolution is too strong to be ignored. Lyn investigated the coupling mechanism between the flow movement and sediment transport with rapid changing upstream boundary. He concluded that decoupled models led to ill-posed problems as general boundary conditions cannot be satisfied. Holly and Rahuel further reported that there existed an upper limit on the time step in decoupled models. Cao et al. conducted the analysis on coupled and decoupled models by simplified continuity equations and asynchronous solution procedure. Valuable conclusions they obtained show that simplification of flow equations has negligible effects on degradation. However, errors due to the simplification could be significant during process of aggradation.

To suppress numerical errors or instabilities associated with the decoupled models, some researchers adopted the semicoupled models and fully coupled models and the simulation results were reasonably satisfying. Some semicoupled models both gives the possibility to have results similar to those obtained using fully-coupled models/analytical solutions/experiments and needs reduced computational times, comparable to those needed by a decoupled model [22,23]. Such an efficiency is reached by constantly updating hydrodynamic and morphodynamic terms without solving a complex equation system. However, the updating is usually implemented in specified situations and its applicability needs to be further calibrated. In addtion, an unavoidable difficulty in the application of fully coupled models is the computational cost is confoundedly high, as the governing equations need to be solved simultaneously and the repeated iteration reduces the efficiency.

Aforementioned discussion briefly focuses on the capability of different types of sediment transport models. It can be well recognized that fully coupled models is inevitable in situations that coupling interaction between flow and sediment is strong. A series of attractive questions come to the authors' mind: what is the coupling mechanism? Can the coupling mechanism be explicitly expressed? What roles the coupling mechanism plays in sediment transport models? This paper tries to answer these questions by use of characteristics theory. In reality, the set of governing equations in different sediment transport models constructs a nonlinear hyperbolic system [20,27]. The most fundamental mathematical theory of hyperbolic system is characteristics, which can be illustrated as eigenvalue, eigenvector and characteristic relationship. The characteristics account for the interrelations between variables in the hyperbolic system [28].

The present work aims to explore the coupling mechanism between flow movement, sediment transport and riverbed evolution in mathematical models for sediment transport based on the characteristics theory. Firstly, currently widely used mathematical models for sediment transport were integrally summarized. Secondly, eigenvalues, eigenvectors and characteristic relationships of all these models were deducted by the method of singular perturbation technology. Finally, qualitative and quantitative analysis of coupling mechanism was conducted.

2 Models for sediment transport

2.1 Governing equations

Consider one-dimensional motion in an open channel flow with rectangular cross sections of unit width and erodible riverbed composed of uniform sediment. The motion of flow, sediment transport and riverbed adjustment can be modeled by the shallow water equations (eqs. (1)–(4)), the non-equilibrium sediment transport equation (eq. (5)) and the bed evolution equation (eqs. (6) and (7)), respectively. These governing equations are shown in Table 1.

Eqs. (2) and (4) are the modified Saint-Venant's continuity and momentum equations (eqs. (1) and (3)), respectively, taking into account the effect of the suspended load transport and bed morphology [4,15]. The last term on the left-hand side (LHS) of eq. (2) represents the effect of bed mobility. The last two terms on LHS of eq. (4) represent spatial variations in suspended sediment concentration, and momentum transfer due to sediment exchange between the flow and the erodible bed, respectively. These three terms are generally neglected in the widely utilized shallow water continuity and momentum equations, based on the assumption that the rate of bed morphological evolution is of a lower order of magnitude than flow changes with adequately

Table 1 Governing equations

Name	Equations	
Flow continuity	$\frac{\partial h}{\partial t}+\frac{\partial (hu)}{\partial x}=0$	(1)
Flow continuity	$\frac{\partial h}{\partial t}+\frac{\partial (hu)}{\partial x}+\frac{\partial z_b}{\partial t}=0$	(2)
Flow motion	$\frac{\partial hu}{\partial t}+\frac{\partial}{\partial x}\left(hu^2+\frac{1}{2}gh^2\right)=gh(i_0-i_f)$	(3)
Flow motion	$\frac{\partial (hu)}{\partial t}+\frac{\partial}{\partial x}\left(hu^2+\frac{1}{2}gh^2\right)+gh\frac{\partial z_b}{\partial x}+\frac{(\rho_s-\rho_w)}{\rho_m}\frac{gh^2}{2}\frac{\partial s_v}{\partial x}-\frac{\rho_b-\rho_m}{\rho_m}u\frac{\partial z_b}{\partial t}=-ghi_f$	(4)
Sediment transport	$\frac{\partial hs_v}{\partial t}+\frac{\partial hus_v}{\partial x}+(1-p)\frac{\partial z_b}{\partial t}=0$	(5)
Bed deformation	$(1-p)\frac{\partial z_b}{\partial t}=\alpha_c\omega(s_v-s_{v*})$	(6)
Bed deformation	$(1-p)\frac{\partial z_b}{\partial t}+\frac{\partial g_b}{\partial x}=\alpha_c\omega(s_v-s_{v*})$	(7)

low sediment concentration. However, the impact of these terms remains to be determined for fluvial processes featuring active suspended sediment transport and rapid bed deformation [29].

For the bed evolution equation, eq. (6) considers the transport of suspended load, and eq. (7) considers the transport of total sediment load (suspended load and bed-load).

Where h=flow depth; t=time; u=velocity of flow; x= streamwise coordinate; z_b=bed elevation; i_0=bed slope; g=gravitational acceleration; i_f = friction slope; ρ_s = density of sediment; ρ_w=density of water; p=bed sediment porosity; ρ_m= density of water-sediment mixture, $\rho_m=\rho_s s_v/\rho_s+\rho_w\left(1-s_v/\rho_s\right)$; s_v=volumetric sediment concentration; ρ_b=density of saturated bed, ρ_b= $(1-p)\rho_s+p\rho_w$; s_{v*}= volumetric capacity of suspended load; α_c= adaption coefficient of suspended load; ω= sediment settling velocity; g_b=volumetric capacity of bed-load transport.

2.2 Models summary

According to the governing equations, the various types of models for sediment transport are summarized in Table 2. A total-sediment transport model that employs eqs. (2), (4), (5) and (7) is denoted TM. A bed-load transport model that employs eqs. (2), (4), and (7)* is denoted BM. A so-defined coupled suspended-load transport model that employs the complete shallow water equations (eqs. (2) and (4)), eqs. (5) and (6) is denoted SCM, compared to a decoupled suspended-load transport model that employs the simplified shallow water equations (eqs. (1) and (3)), eqs. (5) and (6). The decoupled suspended-load transport model is denoted SDM. It is obvious that difference between the SCM and SDM is the simplification in the shallow water equations. Strictly speaking, a coupled model should employ the complete equations with synchronous procedure. However, the present work mainly focuses on the hyperbolic nature of models and the procedure of numerical solution is not considered.

Table 2 Model summary

Models	Denotation	Governing equations
Total-sediment Transport	TM	(2), (4), (5), (7)
Bed-load Transport	BM	(2), (4), (7)*
Suspended-load Transport	SDM	(1), (3), (5), (6)
Suspended-load Transport	SCM	(2), (4), (5), (6)

Note: in governing equations for bed-load transport, RHS of eq. (7) equals to zero, as denoted eq. (7)*.

It is necessary to emphasize that the models discussed in the present work are capacity models. Noncapacity models (e.g., refs. [29–32]) which incorporate the sediment entrainment and deposition fluxes instead of sediment transport capacity are also used to simulate flow and sediment transport in alluvial rivers. Consider that the applicability of non-capacity model has so far remained to be determined, the capacity models are considered in this research as they are generally used in most existing models for sediment transport (e.g., refs. [1,2,33–35]).

2.3 Empirical relationships

To close these models, several coefficients need to be empirically determined. The friction slope is evaluated by applying Manning's formula, namely

$$i_f=\frac{n^2u^2}{h^{4/3}}, \tag{8}$$

where n=Manning's roughness coefficient.

A formula proposed by Zhang is used to compute the sediment transport capacity, which is given as

$$s_{v*} = k_s \left(\frac{u^3}{gh\omega} \right)^{m_s}, \tag{9}$$

where k_s and m_s are two empirical parameters, k_s = 0.452 kg/m^3 and m_s =0.762.

The adaption coefficient of suspended load α_c is defined as the ratio between the reference concentration near the riverbed and the depth averaged concentration in the flow. Several empirical approaches have been proposed in the literature for determining the value of α_c [36–38]. It has been found that α_c ranges from 0.001 in the case of deposition to 1.0 for erosion. This paper treats α_c as 1.0.

For capacity of bed-load transport, we follow Cunge et al. and adopt the form

$$g_b = k_b u^{m_b} h^{n_b}, \tag{10}$$

where k_b depends upon the local flow conditions and characteristics of sediment; m_b and n_b are constants. It has demonstrated that $1 \leqslant m_b, n_b \leqslant 2$ for slowly varying alluvial flows [39,40]. Most of the existing sediment transport functions are reasonably well approximated by taking k_b as constant in eq. (10). For simplicity this approximation is adopted in the present research. Furthermore, it is readily observed that qualitative nature of the results obtained in the present work are unchangeable with various forms of g_b, provided that it remains as a positive, monotone increasing function of *u* and *h*.

3 Characteristics of sediment transport models

The set of governing equations in aforementioned sediment transport models constructs a nonlinear hyperbolic system. One of the most fundamental theories of hyperbolic system is the characteristics, which can be illustrated as eigenvalues, eigenvectors and characteristic relationships [28]. The characteristics mathematically and explicitly describe the interaction between each variable in the nonlinear system and the property of disturbance propagation, avoiding the great difficulty in obtaining the analytic solutions to the nonlinear system. Therefore, analysis on the hyperbolic nature (i.e., eigenvalues, eigenvectors and characteristic relationships) of sediment transport models is an attractive alternative approach to investigate the complex interactions between flow movement, sediment transport and riverbed evolution in alluvial rivers.

In this paper, we select the model of total-sediment transport as the typical example and deduct eigenvalues, eigenvectors and characteristic relationships in detailed process. The analysis of other models will remain to follow the similar procedure.

3.1 Total-sediment transport

With a constant flow depth h_0, flow velocity u_0 , and sediment concentration s_{v0}, the most simple solution of eqs. (2), (4), (5) and (7) is that representing a uniform flow with equilibrium sediment transport down an incline of slope i_0, where $\partial z_b / \partial t$ =0. After substitution into eqs. (2), (4), (5) and (7), we obtain the following expressions:

$$i_0 = \frac{n^2 u_0^2}{h_0^{4/3}}, s_{v0} = s_{v*0} = k_s \left(\frac{u_0^3}{gh_0\omega} \right)^{m_s}, g_{b0} = k_b u_0^{m_b} h_0^{n_b}. \tag{11}$$

Typical scales for fluid depth, velocity and sediment concentration are h_0, u_0 and s_{v*0}, respectively. Also, with a time scale t_0, a typical horizontal length scale in the flow is given by $l_0 = u_0 t_0$ ($l_0 \gg h_0$). We use these scales to introduce the following dimensionless variables, $h = h_0 h'$, $u = u_0 u'$, $z_b = h_0 \xi'$, $x = l_0 x'$, $t = t_0 t'$, $\omega = u_0 \omega'$, $s_v = s_{v*0} s_v'$, $g_b = g_{b0} g_v'$. After dropping primes for convenience, eqs. (2), (4), (5) and (7) become in dimensionless form

$$\frac{\partial h}{\partial t} + \frac{\partial (hu)}{\partial x} + \frac{\partial \xi}{\partial t} = 0, \tag{12}$$

$$\begin{aligned} &\frac{\partial u}{\partial t} + u\frac{\partial u}{\partial x} + \frac{1}{F_0^2}\frac{\partial h}{\partial x} + \frac{1}{F_0^2}\frac{\partial \xi}{\partial x} + \frac{\rho_s - \rho_w}{2\rho_m}\frac{h}{F_0^2}\frac{\partial s_v}{\partial x} \\ &- \frac{\rho_b}{\rho_m}\frac{u}{h}\frac{\partial \xi}{\partial t} = \frac{g(i_0 - i_f)l_0}{F_0^2 h_0}, \end{aligned} \tag{13}$$

$$\frac{\partial hs_v}{\partial t} + \frac{\partial hus_v}{\partial x} + (1-p)\frac{\partial \xi}{\partial t} = 0, \tag{14}$$

$$\frac{\partial \xi}{\partial t} + \varepsilon_b \frac{\partial u^{m_b} h^{n_b}}{\partial x} = \frac{l_0 \alpha_c \omega}{h_0 (1-p)} \left(s_v - s_{*v0} \left(\frac{u^3}{h} \right)^{m_s} \right), \tag{15}$$

where $F_0 = \sqrt{u_0^2 / (gh_0)}$ is the Froude number of the uniform flow. $\varepsilon_b = g_{b0} / (h_0 u_0)$ measures the ratio of overall sediment to fluid discharge in the uniform flow. ε_b in itself could be denoted as the influence of sediment transport on flow routing.

In terms of the dimensionless variables, the uniform flow with equilibrium sediment transport becomes

$$h = 1, \quad u = 1, \quad \xi = 0, \quad s_v = 1. \tag{16}$$

The governing eqs. (12)–(15) can be cast in the following vector form:

$$\boldsymbol{A}\frac{\partial \boldsymbol{Y}}{\partial t}+\boldsymbol{B}\frac{\partial \boldsymbol{Y}}{\partial x}=\boldsymbol{W}, \tag{17}$$

where $\boldsymbol{Y}=\left[h,u,s_v,\xi\right]^{\mathrm{T}}$ is an admissible classical solution, and $\boldsymbol{A}$, $\boldsymbol{B}$ are the matrices,

$$\boldsymbol{A}=\begin{bmatrix} 1 & 0 & 0 & 1 \\ 0 & 1 & 0 & \beta_1 \\ s_v & 0 & h & 1-p \\ 0 & 0 & 0 & 1 \end{bmatrix};$$

$$\boldsymbol{B}=\begin{bmatrix} u & h & 0 & 0 \\ 1/F_0^2 & u & \beta_2 & 1/F_0^2 \\ us_v & hs_v & hu & 0 \\ \varepsilon_b n_b h^{n_b-1}u^{m_b} & \varepsilon_b m_b u^{m_b-1}h^{n_b} & 0 & 0 \end{bmatrix};$$

$$\boldsymbol{W}=\left[0,\frac{g(i_0-i_f)l_0}{F_0^2 h_0},0,\frac{l_0\alpha_c\omega}{h_0(1-p)}\left(s_v-s_{*v0}\left(\frac{u^3}{h}\right)^{m_s}\right)\right]^{\mathrm{T}};$$

$$\beta_1=-\rho_b u/(\rho_m h);\ \ \beta_2=(\rho_s-\rho_w)h/\left(2F_0^2\rho_m\right).$$

3.1.1 Eigenvalues

Based on the theory of Linear Algebra, eigenvalues of the hyperbolic system that the partial differential eq. (17) constructs can be determined by the equality

$$\det\left(\boldsymbol{A}^{-1}\boldsymbol{B}-\lambda\boldsymbol{I}\right)=0, \tag{18}$$

where $\boldsymbol{I}$ is the unit matrix, λ denotes the eigenvalue.

It is readily observed that expansion of LHS of eq. (18) arrives at a four-order polynomial function of independent variable λ, and the explicit form of λ is difficult to be obtained. Consider that ε_b actually can be recognized as a small disturbance of bed-load sediment transport imposed upon uniform flow movement, its magnitude is of a lower order (i.e., $\varepsilon_b \ll 1$) compared to that of flow [40,41]. In this study, the singular perturbation method is implemented to obtain the asymptotic solutions of eq. (18) [42].

Four eigenvalues of nonlinear hyperbolic system eq. (17) are λ_i (i =1, 2, 3, 4), as shown in eqs. (19)–(22). It is obvious that λ_i (i =1, 2, 3, 4) depend only upon variables u, h and ε_b. We note that in the limit $\varepsilon_b \to 0$, eqs. (19)–(22) formally reduce to those of fixed bed hydraulics. Especially, λ_1 and λ_4 have "revised forms" of two eigenvalues of the conventional Saint-Venant's equations (for which $\lambda_1=u-\sqrt{h}/F_0$ and $\lambda_4=u+\sqrt{h}/F_0$. The "revised forms" of λ_1 and λ_4 involve parameters (i.e., s_v, m_b, and n_b) which describe the total sediment transport. Therefore, it exclusively implies that the property of flow moment is influenced by the total sediment transport.

$$\lambda_1 \sim \begin{cases} \left(u-\sqrt{h}/F_0\right) \\ \times\left[1+0.5\varepsilon_b h^{n_b-2}u^{m_b-1}F_0^2\eta_1/\left(u-\sqrt{h}/F_0\right)^2+O(\varepsilon_b^2)\right], \\ \quad u<\sqrt{h}/F_0+O(\sqrt{\varepsilon_b}), \\ 0.5\sqrt{\varepsilon_b}\left(\bar{u}-\sqrt{\bar{u}^2+2(m_b-n_b)h^{n_b+0.5m_b-0.5}/F_0^{m_b+1}}\right) \\ +O(\varepsilon_b),\ u=\sqrt{h}/F_0\pm O(\sqrt{\varepsilon_b}), \\ \varepsilon_b(m_b-n_b)h^{n_b}u^{m_b}/\left[F_0^2\left(h/F_0^2-u^2\right)\right]+O(\varepsilon_b^2), \\ \quad u>\sqrt{h}/F_0+O(\sqrt{\varepsilon_b}), \end{cases} \tag{19}$$

$$\lambda_2 \sim \begin{cases} \varepsilon_b(m_b-n_b)h^{n_b}u^{m_b}/\left[F_0^2\left(h/F_0^2-u^2\right)\right], \\ \quad u<\sqrt{h}/F_0+O(\sqrt{\varepsilon_b}), \\ 0.5\sqrt{\varepsilon_b}\left(\bar{u}+\sqrt{\bar{u}^2+2(m_b-n_b)h^{n_b+0.5m_b-0.5}/F_0^{m_b+1}}\right) \\ +O(\varepsilon_b),\quad u=\sqrt{h}/F_0\pm O(\sqrt{\varepsilon_b}), \\ \left(u-\sqrt{h}/F_0\right)\left[1+0.5\varepsilon_b h^{n_b-2}u^{m_b-1}F_0^2\eta_1/\left(u-\sqrt{h}/F_0\right)^2\right. \\ \left.+O(\varepsilon_b^2)\right]+O(\varepsilon_b^2),\quad u>\sqrt{h}/F_0+O(\sqrt{\varepsilon_b}), \end{cases} \tag{20}$$

$$\lambda_3 \sim u\left[1+\varepsilon_b n_b h^{n_b-2}u^{m_b-1}\beta_2(1-p-s_v)F_0^2+O(\varepsilon_b^2)\right], \tag{21}$$

$$\lambda_4 \sim \left(u+\sqrt{h}/F_0\right) \times\left[1+0.5\varepsilon_b n_b h^{n_b-2}u^{m_b-1}F_0^2\eta_2\left(u+\sqrt{h}/F_0\right)^{-2}+O(\varepsilon_b^2)\right], \tag{22}$$

where $\bar{u}=\left(u-\sqrt{h}/F_0\right)/\varepsilon_b^{0.5}$,

$$\eta_1=\left[n_b u^2+m_b h/F_0^2-(m_b+n_b)u\sqrt{h}/F_0\right] \times\left[(s_v+p-1)\beta_2+h^{3/2}\beta_1/F_0\right]+m_b u h^{3/2}/F_0^3-n_b u^2 h/F_0^2,$$

$$\eta_2=\left[n_b u^2+m_b h/F_0^2+(m_b+n_b)u\sqrt{h}/F_0\right] \times\left[(s_v+p-1)\beta_2-h^{3/2}\beta_1/F_0\right]-m_b u h^{3/2}/F_0^3-n_b u^2 h/F_0^2,$$

$O(\bullet)$ is a function of "$\bullet$" such that $\lim_{\bullet\to 0} O(\bullet)/\bullet$ =a non-zero constant.

3.1.2 Eigenvectors

To obtain the eigenvector of the hyperbolic system that the partial differential eq. (17) constructs, we denote the left eigenmatrix of $\boldsymbol{A}^{-1}\boldsymbol{B}$ in eq. (18) as

$$\boldsymbol{L}=\left[\boldsymbol{e}_1,\boldsymbol{e}_2,\boldsymbol{e}_3,\boldsymbol{e}_4\right]^{\mathrm{T}}, \tag{23}$$

where $\boldsymbol{e}_i=\left[l_{i1},l_{i2},l_{i3},l_{i4}\right]^{\mathrm{T}}$ is the left eigenvector of matrix $\boldsymbol{A}^{-1}\boldsymbol{B}$ in eq. (18) (associate with the eigenvalues λ_i); l_{ik}

(k =1, 2, 3, 4) is the column vector of matrix $\boldsymbol{A}^{-1}\boldsymbol{B}$.

Based on the theory of Linear Algebra, there exists the relationship

$$\boldsymbol{L}\boldsymbol{A}^{-1}\boldsymbol{B} = \Lambda \boldsymbol{L}, \tag{24}$$

where Λ is the diagonal matrix, which is

$$\Lambda = \begin{bmatrix} \lambda_1 & 0 & 0 & 0 \\ 0 & \lambda_2 & 0 & 0 \\ 0 & 0 & \lambda_3 & 0 \\ 0 & 0 & 0 & \lambda_4 \end{bmatrix}. \tag{25}$$

After expanding eq. (24), the left eigenvector $\boldsymbol{e}_i$ of matrix $\boldsymbol{A}^{-1}\boldsymbol{B}$ (associate with the eigenvalues λ_i for i =1, 2, 3, 4) is readily obtained as eq. (26). We note that in the limit $\varepsilon_b \to 0$, eq. (26) formally reduces to the eigenvector of fixed bed hydraulics.

$$\boldsymbol{e}_i = \left[\frac{F_0^{-2} - \varepsilon_b \beta_1 n_b h^{n_b - 1} u^{m_b} - \varepsilon_b \dfrac{(s_v + p - 1) n_b h^{n_b - 2} u^{m_b} \beta_2}{(u - \lambda_i)} + \varepsilon_b \dfrac{n_b h^{n-1} u^m}{F_0^2 \lambda_i}}{-u + \lambda_i + \varepsilon_b n_b h^{n-1} u^m}, \quad 1, \frac{\beta_2}{\lambda_i - u}, \frac{1}{F_0^2 \lambda_i} \right]^{\mathrm{T}}. \tag{26}$$

3.1.3 Characteristic relationships

With the eigenvalues λ_i (i =1, 2, 3, 4) distinct, the left eigenvectors $\{\boldsymbol{e}_i\}$ (i =1, 2, 3, 4) are linearly independent. After multiplying eq. (17) by the non-singular diagonal matrix Λ, we obtain the equivalent system in canonical form as

$$\begin{aligned} &\left(\frac{F_0^{-2} - \varepsilon_b \beta_1 n_b h^{n_b - 1} u^{m_b} - \varepsilon_b \dfrac{(s_v + p - 1) n_b h^{n_b - 2} u^{m_b} \beta_2}{(u - \lambda_i)} + \varepsilon_b \dfrac{n_b h^{n-1} u^m}{F_0^2 \lambda_i}}{-u + \lambda_i + \varepsilon_b n_b h^{n-1} u^m} \right) \\ &\times \left(\frac{\partial h}{\partial t} + \lambda_i \frac{\partial h}{\partial x} \right) + \left(\frac{\partial u}{\partial t} + \lambda_i \frac{\partial u}{\partial x} \right) \\ &- \frac{\beta_2}{(u - \lambda_i)} \left(\frac{\partial s_v}{\partial t} + \lambda_i \frac{\partial s_v}{\partial x} \right) + \frac{1}{F_0^2 \lambda_i} \left(\frac{\partial \xi}{\partial t} + \lambda_i \frac{\partial \xi}{\partial x} \right) \\ &= \frac{g(i_0 - i_f) l_0}{F_0^2 h_0} + \frac{l_0 \alpha \omega}{F_0^2 h_0 (1 - p) \lambda_i} \left(s_v - s_{*v0} \left(\frac{u^3}{h} \right)^{m_s} \right), \end{aligned} \tag{27}$$

for i =1, 2, 3, 4. There exist four families of characteristic curves upon which each of eq. (27) reduces to an ordinary differential equation. We define the curves in the jth characteristic family (j =1, 2, 3, 4) as $x = x_j(t)$ where

$$\frac{\mathrm{d}x_j}{\mathrm{d}t} = \lambda_j \left(\boldsymbol{Y}(x_j, t) \right). \tag{28}$$

Then the jth equation of eq. (27) could be further expressed in eq. (29).

Eq. (29) is the characteristic relationship of nonlinear hyperbolic system eq. (17) upon the jth characteristic family. By integrating eqs. (28) and (29) along each of the four families of characteristic curves, an analytical solution to eq. (27) can be obtained. More importantly, the characteristic relationship in eq. (29) demonstrates that flow movement, sediment transport and river bed evolution interact with each other. It is attractive to physically explain the "coupled mechanism" between sediment-laden flows and river bed evolution in alluvial rivers with total sediment transport.

$$\begin{aligned} &\left(\frac{F_0^{-2} - \varepsilon_b \beta_1 n_b h^{n_b - 1} u^{m_b} - \varepsilon_b \dfrac{(s_v + p - 1) n_b h^{n_b - 2} u^{m_b} \beta_2}{(u - \lambda_j)} + \varepsilon_b \dfrac{n_b h^{n-1} u^m}{F_0^2 \lambda_j}}{-u + \lambda_j + \varepsilon_b n_b h^{n-1} u^m} \right) \\ &\times \frac{\mathrm{d}h}{\mathrm{d}t} + \frac{\mathrm{d}u}{\mathrm{d}t} - \frac{\beta_2}{(u - \lambda_j)} \frac{\mathrm{d}s_v}{\mathrm{d}t} + \frac{1}{F_0^2 \lambda_j} \frac{\mathrm{d}\xi}{\mathrm{d}t} = \frac{g(i_0 - i_f) l_0}{F_0^2 h_0} \\ &+ \frac{l_0 \alpha \omega}{F_0^2 h_0 (1 - p) \lambda_j} \left(s_v - s_{*v0} \left(\frac{u^3}{h} \right)^{m_s} \right). \end{aligned} \tag{29}$$

3.2 Bed-load transport

Following the above-illustrated procedure, the eigenvalues, eigenvectors and characteristic relationship of model for bed-load transport can be determined, as shown in eqs. (30)–(31), eq. (32) and eq. (33), respectively. Observation from eqs. (30)–(33) indicates that in the limit $\varepsilon_b \to 0$, eqs. (30)–(33) formally reduce to those of fixed bed hydraulics. Differently from the model for total-sediment transport, three families of characteristics existed for bed-load transport model, since the suspended-load transport is not included. More importantly, coupled interactions between flow movement and bed-load transport are also illustrated in the characteristics. In more detail, the property of flow moment is influenced by the bed-load sediment transport, whilst the bed form development is determined by the local flow conditions (i.e., flow depth, flow velocity and flow regime).

Zanre and Needham deducted the hyperbolic nature of model for bed-load transport and they obtained similar, but simplified forms of characteristics, compared to eqs. (30) –(33). It is necessary to note that they neglected the effect of river bed mobility on flow movement and adopted a simpler form of capacity of bed-load transport (i.e., $g_b = k_b u^{m_b}$). Compared to Zanre and Needham's consideration, results in the present work have more representative significance as the effect of bed mobility is coupled in the continuity equations and spatial variations in suspended sediment concentration and momentum transfer due to sediment exchange between the flow and the erodible bed are included in the momentum equations.

3.3 Suspended-load transport

The eigenvalues, eigenvectors and characteristic relationship of hyperbolic systems that SCM and SDM construct are shown in Tables 3–5, respectively. In Table 3, $\lambda_{1,4}$, λ_2 and λ_3 represent the eigenvalues of flow motion, bed deformation and suspended-load transport, respectively. It's obvious that λ_i (i =1, 2, 3, 4) of both SCM and SDM are the same as the fixed bed hydraulics. In other words, the interactions between flow movement, sediment transport, and bed deformation cannot be illustrated in the result of eigenvalues, even for the widely recognized "coupled model" as SCM which employs the complete governing equations.

Observation from Tables 4 and 5 indicates that, the eigenvectors and characteristic relationship for SDM are the same as those of the fixed bed hydraulics. Furthermore, for SCM, the effect of sediment transport and bed evolution on flow motion is illustrated in the eigenvectors and characteristic relationship for the family of flow to certain extent. However, influence of flow movement on suspended-load transport and riverbed adjustment cannot be physically described in the eigenvectors and characteristic relationship for the families of sediment transport and riverbed evolution. For instance, the characteristic relationship along characteristic curve λ_2 of SCM in Table 5 demonstrates that riverbed evolution is only decided by the local sediment concentration and capacity of suspended sediment, not incorporating the key factors of flow conditions (i.e., flow regime, longitudinal variations of flow depth and velocity).

Generally speaking, it is reasonable to consider that either SDM or SCM is decoupled by the analysis of characteristics. The interactions between flow movement, suspended-load transport and riverbed evolution cannot be integrally illustrated in eigenvalues, eigenvectors and characteristic relationship. As previously mentioned, the feedback of riverbed mobility on the flow motion cannot be ignored for fluvial processes featuring active suspended sediment transport and rapid bed deformation [29]. Under these situations, the availability of adopting SCM still needs to be further examined.

$$\lambda_1 \sim \begin{cases} \left(u-\sqrt{h}/F_0\right) \\ \times\left[1+\varepsilon_b \dfrac{\left(n_b u - m_b\sqrt{h}/F_0\right)\left[(\alpha_c-1)\sqrt{h}/F_0-\alpha_c u\right]}{2F_0^{-1}u^{-m_b}h^{1.5-n_b}\left(u-\sqrt{h}/F_0\right)^2}+O(\varepsilon_b^2)\right], \\ \quad u<\sqrt{h}/F_0+O(\sqrt{\varepsilon_b}), \\ 0.5\sqrt{\varepsilon_b}\left(\bar{u}-\sqrt{\bar{u}^2+2(m_b-n_b)h^{n_b-0.5+0.5m_b}/F_0^{m_b+1}}\right) \\ +O(\varepsilon_b), \quad u=\sqrt{h}/F_0\pm O(\sqrt{\varepsilon_b}), \\ \varepsilon_b h^{n_b}u^{m_b}(m_b-n_b)/\left[F_0^2\left(h/F_0^2-u^2\right)\right]+O(\varepsilon_b^2), \\ \quad u>\sqrt{h}/F_0+O(\sqrt{\varepsilon_b}), \end{cases} \tag{30}$$

$$\lambda_2 \sim \begin{cases} \varepsilon_b h^{n_b}u^{m_b}(m_b-n_b)/\left[F_0^2\left(h/F_0^2-u^2\right)\right]+O(\varepsilon_b^2), \\ \quad u<\dfrac{\sqrt{h}}{F_0}+O(\sqrt{\varepsilon_b}), \\ 0.5\sqrt{\varepsilon_b}\left(\bar{u}+\sqrt{\bar{u}^2+2(m_b-n_b)h^{n_b-0.5+0.5m_b}/F_0^{m_b+1}}\right)+O(\varepsilon_b), \\ \quad u=\sqrt{h}/F_0\pm O(\sqrt{\varepsilon_b}), \\ \left(u-\sqrt{h}/F_0\right) \\ \times\left[1+\varepsilon_b \dfrac{\left(n_b u - m_b\sqrt{h}/F_0\right)\left[(\alpha_c-1)\sqrt{h}/F_0-\alpha_c u\right]}{2F_0^{-1}u^{-m_b}h^{1.5-n_b}\left(u-\sqrt{h}/F_0\right)^2} \right. \\ \quad \left. +O(\varepsilon_b^2)\right], \quad u>\sqrt{h}/F_0+O(\sqrt{\varepsilon_b}), \end{cases} \tag{31}$$

Table 3 Eigenvalues of models for suspended-load transport

Models	Eigenvalues
SDM	$\lambda_{1,4}=u\pm\sqrt{gh}$ $\lambda_2=0$ $\lambda_3=u$
SCM	$\lambda_{1,4}=u\pm\sqrt{gh}$ $\lambda_2=0$ $\lambda_3=u$

Table 4 Eigenvectors of models for suspended-load transport

Models	Eigenvectors
SDM	$\boldsymbol{R}=\begin{bmatrix} -\dfrac{h}{\sqrt{gh}} & 0 & 0 & \dfrac{h}{\sqrt{gh}} \\ 1 & 0 & 0 & 1 \\ 0 & 0 & 1 & 0 \\ 0 & 1 & 0 & 0 \end{bmatrix}$
SCM	$\boldsymbol{R}=\begin{bmatrix} -\dfrac{h}{\sqrt{gh}} & \dfrac{gh}{u^2-gh} & -\dfrac{(\rho_s-\rho_w)h}{2\rho_m} & \dfrac{h}{\sqrt{gh}} \\ 1 & \dfrac{gu}{gh-u^2} & 0 & 1 \\ 0 & 0 & 1 & 0 \\ 0 & 1 & 0 & 0 \end{bmatrix}$

Note: $\boldsymbol{R}$ is the matrix of the right eigenvectors.

Table 5 Characteristic relationship of models for suspended-load transport

Models	Characteristic relationship
SDM	$\begin{cases} -\dfrac{\sqrt{gh}}{h}\dfrac{\mathrm{d}h}{\mathrm{d}t}\Big\|_{\lambda_1}+\dfrac{\mathrm{d}u}{\mathrm{d}t}\Big\|_{\lambda_1}=g\left(i_0-i_f\right), \\ \dfrac{\mathrm{d}z_b}{\mathrm{d}t}\Big\|_{\lambda_2}=\dfrac{\alpha_c\omega\left(s_v-s_{*v}\right)}{1-p}, \\ \dfrac{\mathrm{d}s_v}{\mathrm{d}t}\Big\|_{\lambda_3}=-\dfrac{\alpha_c\omega\left(s_v-s_{*v}\right)}{h}, \\ \dfrac{\sqrt{gh}}{h}\dfrac{\mathrm{d}h}{\mathrm{d}t}\Big\|_{\lambda_4}+\dfrac{\mathrm{d}u}{\mathrm{d}t}\Big\|_{\lambda_4}=g\left(i_0-i_f\right), \end{cases}$
SCM	$\begin{cases} -\dfrac{\sqrt{gh}}{h}\dfrac{\mathrm{d}h}{\mathrm{d}t}\Big\|_{\lambda_1}+\dfrac{\mathrm{d}u}{\mathrm{d}t}\Big\|_{\lambda_1}-\dfrac{\rho_s-\rho_w}{\rho_m}\dfrac{\sqrt{gh}}{2}\dfrac{\mathrm{d}s_v}{\mathrm{d}t}\Big\|_{\lambda_1}+\dfrac{g}{u-\sqrt{gh}}\dfrac{\mathrm{d}z_b}{\mathrm{d}t}\Big\|_{\lambda_1}=\dfrac{\alpha_c\omega\left(s_v-s_{*v}\right)}{(1-p)h}\left(\dfrac{\rho_b}{\rho_m}u-\dfrac{\rho_s-\rho_w}{\rho_m}\dfrac{s_v\sqrt{gh}}{1-p}+\dfrac{u\sqrt{gh}}{u-\sqrt{gh}}\right)-gi_f, \\ \dfrac{\mathrm{d}z_b}{\mathrm{d}t}\Big\|_{\lambda_2}=\dfrac{\alpha_c\omega\left(s_v-s_{*v}\right)}{1-p}, \\ \dfrac{\mathrm{d}s_v}{\mathrm{d}t}\Big\|_{\lambda_3}=-\dfrac{s_v\alpha_c\omega\left(s_v-s_{*v}\right)}{(1-p)h}, \\ \dfrac{\sqrt{gh}}{h}\dfrac{\mathrm{d}h}{\mathrm{d}t}\Big\|_{\lambda_4}+\dfrac{\mathrm{d}u}{\mathrm{d}t}\Big\|_{\lambda_4}+\dfrac{\rho_s-\rho_w}{\rho_m}\dfrac{\sqrt{gh}}{2}\dfrac{\mathrm{d}s_v}{\mathrm{d}t}\Big\|_{\lambda_4}+\dfrac{g}{u+\sqrt{gh}}\dfrac{\mathrm{d}z_b}{\mathrm{d}t}\Big\|_{\lambda_4}=\dfrac{\alpha_c\omega\left(s_v-s_{*v}\right)}{(1-p)h}\left(\dfrac{\rho_b}{\rho_m}u+\dfrac{\rho_s-\rho_w}{\rho_m}\dfrac{s_v\sqrt{gh}}{1-p}-\dfrac{u\sqrt{gh}}{u+\sqrt{gh}}\right)-gi_f. \end{cases}$

$$\lambda_3\sim\left(u+\sqrt{h}/F_0\right)\times\left[1+\varepsilon_b\frac{\left(n_bu+m_b\sqrt{h}/F_0\right)\left[\left(\alpha_c-1\right)\sqrt{h}/F_0+\alpha_cu\right]}{2F_0^{-1}u^{-m_b}h^{1.5-n_b}\left(u+\sqrt{h}/F_0\right)^2}+\mathrm{O}(\varepsilon_b^2)\right], \tag{32}$$

$$\boldsymbol{e}_i=\left[1,\frac{\left(\lambda_i+\varepsilon_bn_bu^{m_b}h^{n_b-1}-u\right)F_0^2\lambda_i}{\lambda_i+F_0^2\lambda_i\alpha_c\varepsilon_bn_bu^{m_b+1}h^{n_b-2}+\varepsilon_bn_bu^{m_b}h^{n_b-1}},\frac{\lambda_i+\varepsilon_bn_bu^{m_b}h^{n_b-1}-u}{\lambda_i+F_0^2\lambda_i\alpha_c\varepsilon_bn_bu^{m_b+1}h^{n_b-2}+\varepsilon_bn_bu^{m_b}h^{n_b-1}}\right]^{\mathrm{T}} \tag{33}$$

$$\frac{\mathrm{d}h}{\mathrm{d}t}+\frac{\left(\lambda_i+\varepsilon_bn_bu^{m_b}h^{n_b-1}-u\right)F_0^2\lambda_i}{\lambda_i+F_0^2\lambda_i\alpha_c\varepsilon_bn_bu^{m_b+1}h^{n_b-2}+\varepsilon_bn_bu^{m_b}h^{n_b-1}}\frac{\mathrm{d}u}{\mathrm{d}t}+\frac{\lambda_i+\varepsilon_bn_bu^{m_b}h^{n_b-1}-u}{\lambda_i+F_0^2\lambda_i\alpha_c\varepsilon_bn_bu^{m_b+1}h^{n_b-2}+\varepsilon_bn_bu^{m_b}h^{n_b-1}}\frac{\mathrm{d}\xi}{\mathrm{d}t}=-\frac{\left(\lambda_i+\varepsilon_bn_bu^{m_b}h^{n_b-1}-u\right)F_0^2\lambda_it_0gi_f}{\left(\lambda_i+F_0^2\lambda_i\alpha_c\varepsilon_bn_bu^{m_b+1}h^{n_b-2}+\varepsilon_bn_bu^{m_b}h^{n_b-1}\right)u_0}. \tag{34}$$

4 Analysis of coupling mechanism

Previously obtained characteristics of sediment transport models indicate that interactions between flow movement, sediment transport and bed evolution are coupled in total-sediment transport model and bed-load transport model. It's well attractive to deduce that variations of magnitude of sediment transport and bedform development will play a non-neglectful role on the property of flow motion. The present work chooses the total-sediment transport model as the representative to further explore the coupling mechanism.

4.1 Qualitative analysis

Observation from eqs. (19)–(22) obviously tells that eigenvalues of four families of characteristics of total-sediment transport model are not only related to the flow conditions, but also depend on the sediment transport and riverbed deformation. A qualitative sketch of λ_i (i =1, 2, 3, 4) against u for fixed h is given in Figure 1. And a sketch of λ_i (i =1, 2, 3, 4) against F_0 is shown in Figure 2. It further indicates that there are three waves which propagate downstream for all parameter values. Two of these waves (λ_3, λ_4) propagate faster than the uniform flow speed, whilst λ_2 is slower. The remaining wave λ_1 always propagates upstream.

For λ_1 and λ_2 there exists a transition region in the first quadrant of the (u,h) plane, when $u=\sqrt{h}/F_0\pm\mathrm{O}(\sqrt{\varepsilon_b})$. This means that propagation speeds of the flow moving upstream and riverbed development will present essential changes when the local flow regime varies from subcritical flow to supercritical flow. For subcritical flows (i.e., in regions where $u<\sqrt{h}/F_0$), λ_2 represents the main bedform development propagating locally downstream, whilst for supercritical flow (i.e., in regions where $u>\sqrt{h}/F_0$) , the bedform develops locally upstream through λ_1. For the critical flows (i.e., in regions where

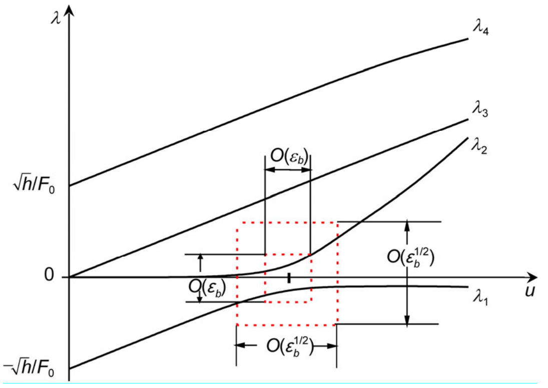

Figure 1 (Color online) The eigenvalues λ_i (i=1, 2, 3, 4) in the (λ,u) plane.

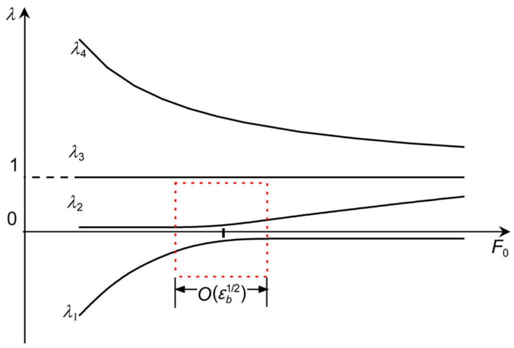

Figure 2 (Color online) The eigenvalues λ_i (i=1, 2, 3, 4) as functions of F_0 with ε_b of $O(1)$.

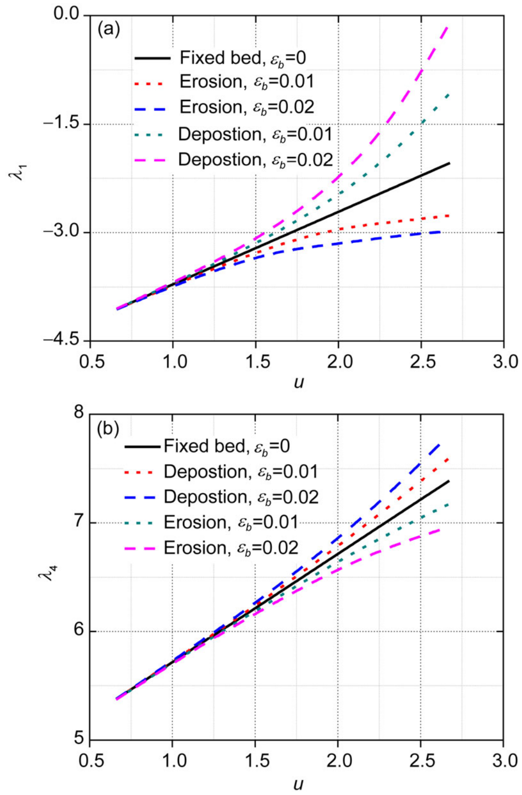

Figure 3 (Color online) (a) Variation of speed of flow propagating upstream λ_1 against u with different ε; (b) variation of speed of flow propagating downstream λ_4 against u with different ε.

$u \sim \sqrt{h}/F_0 \pm O(\sqrt{\varepsilon_b})$), the bedform develops upstream and downstream more rapidly, through both of the λ_1 and λ_2 characteristic family.

By eqs. (19) –(33) it is further informed that the bed deformation evolution is mainly determined by the magnitude $O(1)$. λ_3 and λ_4 have a weak effect on the evolution of river bed deformation as they are of the order $O(1)$.

4.2 Quantitative analysis

To quantify the effect on flow movement by sediment transport in total-sediment transport model, variations of eigenvalues with different sediment transport intensity and different suspended-load concentration are studied. Consider a subcritical uniform flow with erodible bed composed of noncohesive uniform sediment particles of diameter D = 0.003 mm, fluid depth scale h_0 is 3 m, flow depth velocity scale u_0 is 1.5 m/s and sediment capacity scale s_{v*0} can be calculated from eq. (11) as 2.90 (for simplicity, $m_b = n_b$ =2). The effects on flow motion by different magnitude of sediment transport intensity in both situations of deposition and erosion are shown in Figure 3. As aforementioned, ε_b could be denoted as the disturbance on flow movement due to total-sediment transport, thus it can be reasonably deduct that the larger ε_b is, the higher interference level is. With u increases, flow motion waves with speeds λ_1 and λ_4 propagate faster with depositing strength increases. However, in situation of erosion, both of λ_1 and λ_4 will decrease when the scouring strength increases. These conclusions could be used to well explain the unusual phenomenon of hyper-concentrated flood propagation in alluvial rivers (e.g. peak discharge increasing during flood routing in lower reaches of Yellow River). In the process of hyper-concentrated flood propagating, the riverbed usually experiences erosion in the former-phase of the flooding due to strong flow strength. Riverbed evolution, however, will present deposition in the post-phase of the flooding as the gradually accumulated sediment concentration in the flow exceeds the sediment carrying capacity [43]. Based on the results obtained in the present work, the post-phase of the flooding moves faster and chases up the former-phase flood propagating at lower speed, and the phenomenon of peak discharge increasing could be reasonably explained.

In addition, as shown in Figure 4, the suspended sediment concentration s_v will also play a significant role on flow routing. The higher suspended sediment concentration is, the faster that the flow propagates both upstream and downstream. This result is consistent with the conclusions in situations of sediment transport intensity. It is necessary to note that, varying values of suspended sediment concentration s_v in Figure 4 are actually set as different referenced equilibrium concentrations.

Generally, in total-sediment transport model, both of sediment transport intensity and suspended-load concentration will play a significant role on the property of flow movement. Therefore, the coupling mechanism between flow motion, sediment transport and riverbed evolution needs to be emphasized and quantitatively determined in mathematical modeling and practical engineering.

Variation of speed of flow propagating downstream λ_4 against u with various concentration of suspended load s_v .

5 Conclusion

In this paper, the coupling mechanism between flow movement, sediment transport and riverbed evolution in mathematical models for sediment transport is studied based on the characteristics theory. Analytic forms of eigenvalues, eigenvectors and characteristic relationships of total-sediment transport model, bed-load transport model and suspened-load transport model are derived, respectively. Effects on flow movement by various sediment transport density are quantitatively analyzed.

Four families of characteristics exist in total-sediment transport model. The eigenvalues λ_1 and λ_4 of flow motion involve sediment parameters as s_v , m_b , n_b , and etc. It exclusively implies that the property of flow moment is influenced by the total sediment transport. The characteristic relationship in eq. (29) demonstrates that variables interact with each other. It physically explains the coupling mechanism between sediment-laden flows and river bed evolution. High total-sediment transport intensity and significant riverbed change will inevitably affect the property of flow movement. In the process of deposition, sediment-laden flow will move faster when sediment transport intensity becomes stronger. In contrast, the wave of flow will propagate at slower speed as erosion intensity becomes stronger.

Differently from total-sediment transport model, there exist three families of characteristics in model for bed-load transport. Coupling interactions between flow movement and bed-load transport are illustrated in the characteristics.

For suspended-load transport models, either SDM or SCM is decoupled by the analysis of characteristics. The interactions between flow movement, suspended-load transport and riverbed evolution cannot be integrally illustrated in eigenvalues, eigenvectors and characteristic relationship. Therefore, the availability of adopting suspended-load transport models in simulation of active sediment transport and rapid bed deformation needs to be further examined.

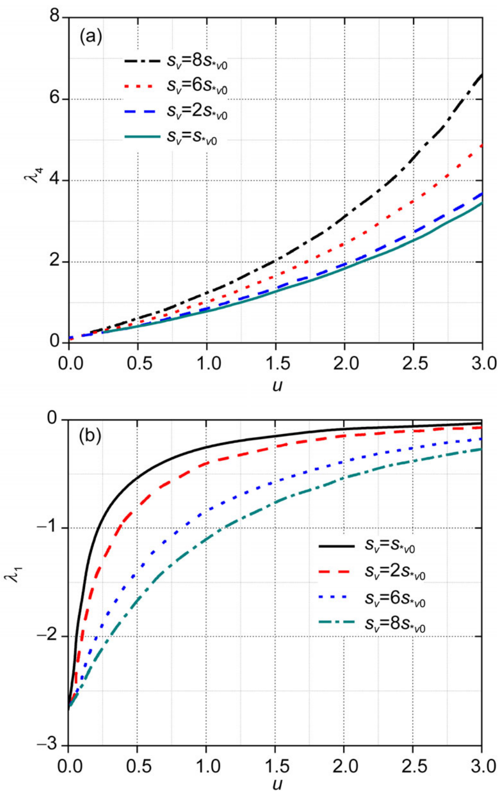

Figure 4 (Color online) (a) Variation of speed of flow propagating upstream λ_1 against $u$with various concentration of suspended load s_v; (b).

This work was supported by the National Key Research and Development Program of China (Grant No. 2016YFC0402503), the National Basic Research Program of China ("973" Project) (Grant No. 2011CB403303), and the National Natural Science Foundation of China (Grant Nos. 51109064 & 51479071).

1 Holly F M, Rahuel J L. New numerical/physical framework for mobile-bed modelling, part 1: Numerical and physical principles. J Hydraul Res IAHR, 1990, 28: 401–416
2 Holly F M, Rahuel J L. New numerical/physical framework for mobile-bed modelling, part 2: Test applications. J Hydraul Res IAHR, 1990, 28: 545–564
3 Cui Y, Parker G, Paola C. Numerical simulation of aggradation and downstream fining. J Hydraul Res IAHR, 1996, 34: 195–204
4 Xia J Q, Lin B L, Falconer R A, et al. Modeling dam-break flows over erodible mobile beds using 2D coupled approach. Adv Water Resour, 2010, 33: 171–183
5 Birnir B, Rowlett J. Mathematical models for erosion and the optimal transportation of sediment. Int J Nonlinear Sci Numer Sim, 2013, 14: 323–337
6 Ji C, Ante M, Eldad A, et al. Numerical investigation of particle saltation in the bed-load regime. Sci China Tech Sci, 2014, 57: 1500–1511
7 Ning J G, Wang X, Ma T B, et al. Numerical simulation of shock wave interaction with defomable particle based on pseudoarc-length method. Sci China Tech Sci, 2015, 58: 848–857
8 Qian H L, Cao Z X, Pender G, et al. Well-balanced numerical model-

ling of non-uniform sediment transport in alluvial rivers. Int J Sed Res, 2015, 30: 117–130
9 Zhu F, Dodd N. The morphodynamics of a swash event on an erodible beach. J Fluid Mech, 2015, 762: 110–140
10 Kassem A, Chaudhry M H. Comparison of coupled and semicoupled numerical models for alluvial channels. J Hydraul Eng ASCE, 1998, 124: 794–802
11 Cao Z, Egashira S. Coupled mathematical modelling of alluvial rivers. J Hydrosci Hydraul Eng JSCE, 1999, 17: 71–85
12 Cao Z, Day R, Egashira S. Coupled and uncoupled numerical modeling of flow and morphological evolution in alluvial rivers. J Hydraul Eng ASCE, 2002, 128: 306–321
13 Park I, Jain S C. River-bed profiles with imposed sediment load. J Hydraul Eng ASCE, 1986, 112: 267–280
14 Park I, Jain S C. Numerical solution of degradation of alluvial channel bed. J Hydraul Eng ASCE, 1987, 113: 845–859
15 Correia L R P, Krishnappan B G, Graf W H. Fully coupled unsteady mobile boundary flow model. J Hydraul Eng, 1992, 118: 476–494
16 Saiedi S. Coupled modeling of alluvial flows. J Hydraul Eng ASCE, 1997, 123: 476–494
17 Fraccarollo L, Capart H. Riemann wave description of erosional dam-break flows. J Fluid Mech, 2002, 461: 183–228
18 Kelly D M, Dodd N. Beach face evolution in the swash zone. J Fluid Mech, 2010, 661: 316–440
19 Briganti R, Dodd N, Kelly D M, et al. An efficient and flexible solver for the simulation of the morphodynamics of fast evolving flows on coarse sediment beaches. Int J Numer Method Fluid, 2012, 69: 859–877
20 Cunge J A, Holly F M J, Verwey A. Practical Aspects of Computational River Hydraulics. London: Pitman Advanced Publishing Program, 1980
21 Lyn D A. Unsteady sediment transport modelling. J Hydraul Eng, ASCE, 1987, 113: 1–15
22 Postacchini M, Brocchini M, Mancinelli A, et al. A multi-purpose, intra-wave, shallow water hydro-morphodynamic solver. Adv Water Resour, 2012, 38: 13–26
23 Postacchini M, Othman I K, Brocchini M, et al. Sediment transport and morphodynamics generated by a dam-break swash uprush: coupled vs uncoupled modeling. Coast Eng, 2014, 89: 99–105
24 Sieben J. A theoretical analysis of discontinuous flow with mobile bed. J Hydraul Res IAHR, 1999, 37: 199–212
25 Busnelli M, Stelling G, Larcher M. Numerical morphological modelling of open-check dams. J Hydraul Eng ASCE, 2001, 127: 105–114
26 Wu W, Wang S S Y. One-dimensional modeling of dam-break flow over movable beds. J Hydraul Eng ASCE, 2007, 133: 1021–1042
27 Whitham G B. Linear and Nonlinear Waves. New York: John Wiley & Sons, Interscinece, 1974
28 Leveque R J. Finite Volume Method for Hyperbolic Problems. London: Cambridge University Press, 2002
29 Cao Z X, Hu P, Pender G. Multiple time scales of fluvial processes with bed load sediment and implication for mathematical modeling. J Hydraul Eng, ASCE, 2011, 137: 267–276
30 Cui Y, Parker G. Numerical model of sediment pulses and sediment-supply disturbances in mountain rivers. J Hydraul Eng ASCE, 2005, 131: 646–656
31 Goutiere L, Soares-Frazao S, Savary C, et al. One-dimensional model for transient flows involving bed-load sediment transport and changes in flow regimes. J Hydraul Eng ASCE, 2008, 134: 726–735
32 Cao Z X, Li Y, Yue Z Y. Multiple time scales of alluvial rivers carrying suspended sediment and their implications for mathematical modeling. Adv Water Resour, 2007, 30: 715–729
33 Capart H, Young D L. Formation of a jump by the dambreak wave over a granular bed. J Fluid Mech, 1998, 372: 165–187
34 Duc B M., Wenka T, Rodi W. Numerical modeling of bed deformation in laboratory channels. J Hydraul Eng ASCE, 2004, 130: 894–904
35 Wu W M. Computational River Dynamics. London: Taylor & Francis, 2007
36 Zhang R J, Xie J H. Sedimentation Research in China: Systematic selections (in Chinese). Beijing: China Water Power Press, 1993
37 Zhou J J, Lin B N. One-dimensional mathematical model for suspended sediment by lateral integration. J Hydraul Eng ASCE, 1998, 124: 712–717
38 Ni J R, Zhang H W, Xue A, et al. Modeling of hyperconcentrated sediment-laden floods in lower yellow river. J Hydraul Eng ASCE, 2004, 130: 1025–1032
39 Engelund F, Hansen E. A Monograph on Sediment Transport In Alluvial Streams. Cophenhagen: Teknisk Vorlag, 1967
40 Zanre D D L, Needham D J. On the hyperbolic nature of the equations of alluvial river hydraulics and the equivalence of stable and energy dissipating shocks. Geophys Astrophy Fluid Dyn, 1994, 76: 193–222
41 Needham D J. Wave hierarchies in alluvial river flows. Geophy Astrophys Fluid Dyn, 1990, 51: 167–194
42 Nayfeh A H. Perturbation Methods. New York: Wiley-Interscinece, 1973
43 Li G Y. Analysis on mechanism of peak discharge increasing during flood routing in lower reaches of Yellow River (in Chinese). J Hydrau Eng, 2008, 5: 511–517